Journal of Computational Physics **174,** 405–420 (2001)
doi:10.1006/jcph.2001.6922, available online at http://www.idealibrary.com on IDEAL®

Role of the LBB Condition in Weak Spectral Projection Methods

F. Auteri,* J.-L. Guermond,† and N. Parolini‡

**Dipartimento di Ingegneria Aerospaziale, Politecnico di Milano, Via La Masa, 34, 20158 Milan, Italy,*
†Laboratoire d'Informatique pour la Mécanique et les Sciences de l'Ingénieur, CNRS, BP 133, 91403, Orsay, France; and ‡Departement de Mathématiques, Ecde Polytechnique Fédérale de Lausanne, CH-1015 Lausanne, Switzerland
E-mail: auteri@aero.polimi.it, guermond@limsi.fr, and nicola.parolini@epfl.ch

Received November 3, 2000; revised August 7, 2001

This paper investigates the relevance of the Ladyshenskaya–Babuška–Brezzi condition in spectral projection methods. We consider the stability and convergence properties for a first-order nonincremental projection method and a second-order incremental projection method, both based on a spectral Galerkin–Legendre spatial discretization. We show that the convergence of both projection methods is controlled by the ability of the spectral framework to approximate correctly the *steady Stokes* problem. © 2001 Elsevier Science

1. INTRODUCTION

The approximation of the primitive variable Navier–Stokes equations by means of finite elements or spectral methods must respect the limits set by numerical analysis in the choice of velocity and pressure approximation spaces. One of these limits consists of the compatibility condition known as the inf–sup condition and also referred to in the literature as the LBB condition, from Ladyshenskaya [20], Babuška [4], and Brezzi [8]. The consequence of not satisfying this condition is the appearance of severe spatial oscillations in the pressure field, usually called spurious pressure modes. One way of eliminating these unphysical oscillations is to augment the discrete problem by adding a term proportional to the equation residual, giving a stabilized version of the original algorithm [18]. Another possibility consists of penalizing the solenoidality constraint, as in pseudocompressibility techniques. The methods of the second class usually yield low-order approximation rates since they are not consistent.

In recent years the idea has emerged that Poisson-based projection techniques are stabilized methods and for this reason can be used with spatial interpolations which do not satisfy the LBB condition. Continuing with the work of Guermond [14] and Guermond and

0021-9991/01 $35.00

Quartapelle [17], where it is shown that this idea is not correct for finite elements, the goal of the present paper is to show that this point of view is not correct in the spectral framework also.

The paper is organized as follows. In Section 2, we formulate the Navier–Stokes problem and introduce a Legendre–Galerkin spectral framework for approximating the solution in space. We recall known stability and convergence results. In Section 3, we reformulate in the spectral framework the nonincremental projection technique introduced by Chorin [12, 13] and Temam [31, 32]. We give stability and convergence estimates, and we show numerical results to illustrate these estimates. In Section 4, we study a backward difference formula (BDF) incremental projection method, and we investigate the relevance of the LBB condition for this scheme. The theoretical results derived in Sections 3 and 4 are illustrated using numerical tests reported in Section 5. We finally conclude in Section 6.

2. FORMULATION OF THE PROBLEM

2.1. The Navier–Stokes Equations

We consider the time-dependent incompressible Navier–Stokes equations formulated in terms of velocity $\boldsymbol{u}$ and pressure p, stated as follows. Find $\boldsymbol{u}$ and p (up to a constant) so that

$$\begin{cases} \frac{\partial \boldsymbol{u}}{\partial t} - \nu \nabla^2 \boldsymbol{u} + (\boldsymbol{u} \cdot \boldsymbol{\nabla})\boldsymbol{u} + \boldsymbol{\nabla} p = \boldsymbol{f}, \\ \boldsymbol{\nabla} \cdot \boldsymbol{u} = 0, \\ \boldsymbol{u}_{|\partial\Omega} = 0, \\ \boldsymbol{u}_{|t=0} = \boldsymbol{u}_0, \end{cases} \tag{2.1}$$

where ν is the viscosity, $\boldsymbol{f}$ is a known body force, and $\boldsymbol{u}_0$ is the divergence-free initial velocity field. For simplicity, we assume homogeneous boundary conditions. The fluid domain Ω is assumed to be the square $[-1, +1]^2$. The data are assumed to be regular enough and to satisfy all the compatibility conditions required for a smooth solution to exist for all time.

2.2. Galerkin–Legendre Approximations

2.2.1. *A Brief Review*

Spectral methods are highly accurate approximation techniques which, contrary to finite elements, are based on global polynomial approximations. The applications of spectral methods in CFD are rooted in the pioneering papers of Kreiss and Oliger [19] and Orzag [23]. The reader is referred to the books of Canuto *et al.* [11] and Bernardi and Maday [5] for quite complete reviews on spectral methods. Though spectral methods can be quite easily analyzed within the Galerkin framework, the collocation framework has been quite often preferred to the Galerkin one in practice. Recently, renewed interest in the Galerkin technique has been prompted by the decisive work of Shen [29], where new Legendre polynomial bases for which both the mass matrix and the stiffness matrix are sparse are introduced. The present work is based on Shen's bases.

2.2.2. *The Interpolation Bases*

Let us introduce the finite dimensional space $\boldsymbol{X}_N = (\mathbb{P}_N \otimes \mathbb{P}_N)^2$, where $\mathbb{P}_N$ denotes the set of polynomial of degree less than or equal to N. We approximate velocity in $\boldsymbol{X}_{0,N} =$

$\boldsymbol{X}_N \cap \boldsymbol{H}_0^1(\Omega)$, where $\boldsymbol{H}_0^1(\Omega)$ is the standard notation for the Sobolev space of vector-valued functions that are square integrable, with square integrable first derivatives, and with zero trace on $\partial\Omega$. Pressure is approximated in the space $M_{\hat{N}} = (\mathbb{P}_{\hat{N}} \otimes \mathbb{P}_{\hat{N}}) \cap L_0^2(\Omega)$, where $L_0^2(\Omega) = \{q \in L^2(\Omega);\ \int_\Omega q = 0\}$. The polynomial order N for velocity is in general different from the polynomial order $\hat{N}$ for pressure. The approximation using the spaces $\boldsymbol{X}_{0,N}$ for velocity and $M_{\hat{N}}$ for pressure is referred to in the following by $\mathbb{P}_N/\mathbb{P}_{\hat{N}}$.

To recast (2.1) in a weak form, we consider two different bases for approximating velocity and pressure. For the velocity field satisfying Dirichlet conditions, we adopt the basis introduced by Shen in [29]; to approximate pressure, a convenient basis in two dimensions is obtained by the tensor product of the standard Legendre polynomial basis normalized such that the mass matrix is the identity.

Approximate velocity and pressure are expanded in the double series

$$\boldsymbol{u}_N(t,x,y) = \sum_{n=2}^{N}\sum_{m=2}^{N} L_n^*(x)L_m^*(y)\boldsymbol{U}_{n,m}(t), \tag{2.2}$$

$$p_{\hat{N}}(t,x,y) = \sum_{\hat{n}=0}^{\hat{N}}\sum_{\hat{m}=0}^{\hat{N}} L_{\hat{n}}^\diamond(x)L_{\hat{m}}^\diamond(y)P_{\hat{n},\hat{m}}(t). \tag{2.3}$$

For a detailed description of the two sets of basis functions L^* and $L^\diamond$ the reader is referred to [1].

2.2.3. *Approximation Properties*

To clarify the approximation properties of the spectral framework considered above, let us introduce the following steady Stokes problem. For a smooth solenoidal vector field $\boldsymbol{u}^s$ in $\boldsymbol{H}_0^1(\Omega)$ and a smooth scalar field $p^s \in L_0^2(\Omega)$, find $\boldsymbol{u}_N^s \in \boldsymbol{X}_{0,N}$ and $p_{\hat{N}}^s \in M_{\hat{N}}$ such that

$$\begin{cases} \left(\boldsymbol{\nabla}\boldsymbol{v}_N, \boldsymbol{\nabla}\left(\boldsymbol{u}_N^s - \boldsymbol{u}^s\right)\right) + \left(\boldsymbol{v}_N, \boldsymbol{\nabla}\left(p_{\hat{N}}^s - p^s\right)\right) = 0, \quad \forall \boldsymbol{v}_N \in \boldsymbol{X}_{0,N}, \\ \left(q_{\hat{N}}, \boldsymbol{\nabla}\cdot\boldsymbol{u}_N^s\right) = 0, \quad \forall q_{\hat{N}} \in M_{\hat{N}}, \end{cases} \tag{2.4}$$

where $(\cdot,\cdot)$ denotes either the L^2 or $\boldsymbol{L}^2$ scalar product indifferently.

Well-posedness of this problem depends on satisfying a compatibility condition between the approximation spaces for velocity and pressure. More precisely, let us introduce the following space:

$$Z_{\hat{N}} = \{q_{\hat{N}} \in M_{\hat{N}};\ (q_{\hat{N}}, \boldsymbol{\nabla}\cdot\boldsymbol{v}_N) = 0, \forall \boldsymbol{v}_N \in \boldsymbol{X}_{0,N}\}.$$

For $\hat{N} = N-2$, we have $Z_{\hat{N}} = \{0\}$, whereas for $\hat{N} = N$, $Z_{\hat{N}}$ is a vector space of dimension 8; the reader is referred to Bernardi and Maday [5] for details. Let $L^2(\Omega)/Z_{\hat{N}}$ denote the quotient space of $L^2(\Omega)$ by $Z_{\hat{N}}$ equipped with the norm

$$\|q\|_{L^2(\Omega)/Z_{\hat{N}}} = \inf_{z\in Z_{\hat{N}}} \|q+z\|_{L^2(\Omega)}, \quad \forall q \in L^2(\Omega).$$

We have the following lemma.

LEMMA 1. *There is* $\beta_{N\hat{N}} > 0$ *so that*

$$\forall q_{\hat{N}} \in M_{\hat{N}} \quad \sup_{\boldsymbol{v}_N \in \boldsymbol{X}_{0,N}} \frac{(q_{\hat{N}}, \boldsymbol{\nabla} \cdot \boldsymbol{v}_N)}{\|\boldsymbol{v}_N\|_{\boldsymbol{H}^1(\Omega)}} \geq \beta_{N\hat{N}} \|q_{\hat{N}}\|_{L^2(\Omega)/Z_{\hat{N}}}, \tag{2.5}$$

and

$$\beta_{N\hat{N}} \sim \begin{cases} N^{-1/2} & if\, \hat{N} = N-2, \\ N^{-1} & if\, \hat{N} = N. \end{cases}$$

The reader is referred to Brezzi and Fortin [9, p. 40], Bernardi and Maday [5], or Quarteroni and Valli [24] for a proof. Condition (2.5) is usually called the LBB condition or inf–sup condition [4, 8, 20].

The idea of using $\hat{N} = N - 2$ stems from the work of Maday *et al.* [22] and Rønquist [26], and early applications of this idea can be found in the thesis of Azaiez [3].

The approximation property of the $\mathbb{P}_N/\mathbb{P}_{\hat{N}}$ framework is stated in the following lemma.

LEMMA 2. *If* $\boldsymbol{u}^s \in \boldsymbol{H}^\sigma(\Omega) \cap \boldsymbol{H}_0^1(\Omega)$ *and* $p^s \in H^{\sigma-1}(\Omega) \cap L_0^2(\Omega)$, *then*

$$\|\boldsymbol{u}^s - \boldsymbol{u}_N\|_{\boldsymbol{L}^2(\Omega)} \leq cN^{-\sigma} \left\{ \|\boldsymbol{u}^s\|_{\boldsymbol{H}^\sigma(\Omega)} + \|p\|_{H^{\sigma-1}(\Omega)} \right\}, \tag{2.6}$$

$$\|\boldsymbol{u}^s - \boldsymbol{u}_N\|_{\boldsymbol{H}^1(\Omega)} + \beta_{N\hat{N}} \|p - p_{\hat{N}}\|_{L^2(\Omega)/Z_{\hat{N}}} \leq cN^{1-\sigma} \left\{ \|\boldsymbol{u}^s\|_{\boldsymbol{H}^\sigma(\Omega)} + \|p\|_{H^{\sigma-1}(\Omega)} \right\}. \tag{2.7}$$

Note that the error bound on the velocity does not depend on the inf–sup constant $\beta_{N\hat{N}}$. This striking result is the consequence of a lemma due to Sacchi–Landriani and Vandeven [27]. The choice $\hat{N} = N$ yields a convergent approximation provided pressure is selected in a space that can be identified with the quotient space $M_{\hat{N}}/Z_{\hat{N}}$. A realization of this space can be obtained by adequate a posteriori filtering (see [5, p. 133] for possible filtering strategies).

2.3. Semidiscrete Weak Spectral Approximation

Now let us turn our attention to the time-dependent Navier–Stokes problem (2.1). We consider the following semidiscrete Navier–Stokes problem. For $t \geq 0$, find $\boldsymbol{u}_N \in C^1([0, T]; \boldsymbol{X}_{0,N})$, $p_{\hat{N}} \in C^0([0, T]; M_{\hat{N}})$ such that, for all $\boldsymbol{v}_N \in \boldsymbol{X}_{0,N}$ and all $q_{\hat{N}} \in M_{\hat{N}}$,

$$\begin{cases} (\boldsymbol{v}_N, \boldsymbol{u}_N(t=0)) = (\boldsymbol{v}_N, \boldsymbol{u}_0), \\ \left(\boldsymbol{v}_N, \frac{\partial \boldsymbol{u}_N}{\partial t}\right) + \nu(\boldsymbol{\nabla} \boldsymbol{v}_N, \boldsymbol{\nabla} \boldsymbol{u}_N) + (\boldsymbol{v}_N, (\boldsymbol{u}_N \cdot \boldsymbol{\nabla}) \boldsymbol{u}_N) + (\boldsymbol{v}_N, \boldsymbol{\nabla} p_{\hat{N}}) = (\boldsymbol{v}_N, \boldsymbol{f}), \\ (q_{\hat{N}}, \boldsymbol{\nabla} \cdot \boldsymbol{u}_N) = 0. \end{cases} \tag{2.8}$$

In the light of Lemma 2, we can derive the following theorem in the linear case (the proof for the nonlinear case being technically more involved, unless a skew-symmetric form of the advection term is used).

THEOREM 1. *If* $\boldsymbol{u} \in W^{1,\infty}(0, T; \boldsymbol{H}^\sigma(\Omega))$ *and* $p \in L^\infty(0, T; H^{\sigma-1}(\Omega))$, *we have*

$$\|\boldsymbol{u} - \boldsymbol{u}_N\|_{L^\infty(0,T;\boldsymbol{L}^2(\Omega))} \leq cN^{-\sigma} \left\{ \|\boldsymbol{u}\|_{W^{1,\infty}(0,T;\boldsymbol{H}^\sigma(\Omega))} + \|p\|_{L^\infty(0,T;H^{\sigma-1}(\Omega))} \right\}, \tag{2.9}$$

$$\begin{aligned} &\|\boldsymbol{u} - \boldsymbol{u}_N\|_{L^\infty(0,T;\boldsymbol{H}^1(\Omega))} + \beta_{N\hat{N}} \|p - p_{\hat{N}}\|_{L^\infty(0,T;L^2(\Omega)/Z_{\hat{N}})} \\ &\quad \leq cN^{1-\sigma} \left\{ \|\boldsymbol{u}\|_{W^{1,\infty}(0,T;\boldsymbol{H}^\sigma(\Omega))} + \|p\|_{L^\infty(0,T;H^{\sigma-1}(\Omega))} \right\}. \end{aligned} \tag{2.10}$$

In conclusion, contrary to the finite-element case where the error estimates of velocity depend on the inf–sup constant, the spectral framework yields optimal error estimates that do not depend on this constant. Convergence on pressure is always guaranteed in the quotient space $L^2(\Omega)/Z_{\hat{N}}$ and the error estimate is proportional to $1/\beta_{N\hat{N}}$.

3. THE (NONINCREMENTAL) PROJECTION METHOD

We want to investigate now the consequences of respecting or not the LBB condition in the context of projection methods. First, we describe the Galerkin–Legendre spectral version of the nonincremental fractional-step projection method (Chorin [12, 13] and Temam [31, 32]), then we state stability and convergence results, illustrated numerically in Section 5.

In view of the spectral discretization of interest here, we assume an implicit treatment for the viscous term and an explicit treatment for the nonlinear one. As a consequence, the method will be only conditionally stable and the time-step size must be chosen under a stability restriction.

3.1. Fractional-Step Time Discretization

The projection method of Chorin and Temam is a time-marching algorithm composed of two separate substeps aiming at decoupling the viscous effects from the incompressibility. Using k to denote the time index, two sequences of approximate velocities $(\boldsymbol{u}^k)_{k\geq 0}$ and $(\hat{\boldsymbol{u}}^k)_{k\geq 1}$ and one sequence of approximate pressure $(p^k)_{k\geq 1}$ are computed as follows.

After initialization, $\boldsymbol{u}^0 = \boldsymbol{u}_0$, for each time-step $k \geq 0$, the first substep consists of the following weak problem. Find $\boldsymbol{u}^{k+1} \in \boldsymbol{H}_0^1(\Omega)$ such that

$$\begin{cases} \frac{(\boldsymbol{v}, \boldsymbol{u}^{k+1}) - (\boldsymbol{v}, \hat{\boldsymbol{u}}^k)}{\Delta t} + \nu(\boldsymbol{\nabla v}, \boldsymbol{\nabla u}^{k+1}) = (\boldsymbol{v}, \boldsymbol{f}^{k+1} - (\boldsymbol{u}^k \cdot \boldsymbol{\nabla})\boldsymbol{u}^k), \quad \forall \boldsymbol{v} \in \boldsymbol{H}_0^1(\Omega), \\ \boldsymbol{u}^{k+1}{}_{|\partial\Omega} = 0. \end{cases} \tag{3.1}$$

The second substep consists of projecting $\boldsymbol{u}^{k+1}$ onto the space of solenoidal vector fields with zero normal trace on $\partial\Omega$. This step may take two alternative forms: in the first form, the projection step is a Darcy problem; in the second form it is a Poisson problem for the pressure. In terms of PDEs the two problems are equivalent, but their weak counterparts are different because of the different underlying functional frameworks. More precisely, by introducing the space

$$\boldsymbol{H}_0^{\mathrm{div}}(\Omega) = \{\hat{\boldsymbol{v}} \in \boldsymbol{L}^2(\Omega) \mid \boldsymbol{\nabla} \cdot \hat{\boldsymbol{v}} \in L^2(\Omega),\ \boldsymbol{n} \cdot \hat{\boldsymbol{v}}_{|\partial\Omega} = 0\},$$

the weak formulation of the Darcy problem consists of looking for $\hat{\boldsymbol{u}} \in \boldsymbol{H}_0^{\mathrm{div}}(\Omega)$ and $p^{k+1} \in L_0^2(\Omega)$ such that

$$\begin{cases} \left(\hat{\boldsymbol{v}}, \frac{\hat{\boldsymbol{u}}^{k+1} - i\boldsymbol{u}^{k+1}}{\Delta t}\right) - (\boldsymbol{\nabla} \cdot \hat{\boldsymbol{v}}, p^{k+1}) = 0, \quad \forall \hat{\boldsymbol{v}} \in \boldsymbol{H}_0^{\mathrm{div}}(\Omega), \\ (q, \boldsymbol{\nabla} \cdot \hat{\boldsymbol{u}}^{k+1}) = 0, \quad \forall q \in L_0^2(\Omega), \end{cases} \tag{3.2}$$

where $i : \boldsymbol{H}_0^1(\Omega) \to \boldsymbol{H}_0^{\mathrm{div}}(\Omega)$ is the natural injection. On the other hand, the weak formulation of the Poisson problem consists of looking for $p \in H^1(\Omega) \cap L_0^2(\Omega)$ and $\hat{\boldsymbol{u}} \in \boldsymbol{L}^2(\Omega)$ such

that

$$\begin{cases} (\nabla q, \nabla p^{k+1}) = -(\Delta t)^{-1}(q, \nabla \cdot \boldsymbol{u}^{k+1}), \quad \forall q \in H^1(\Omega) \cap L^2_0(\Omega), \\ \hat{\boldsymbol{u}}^{k+1} = i\,\boldsymbol{u}^{k+1} - \Delta t \nabla p^{k+1}. \end{cases} \tag{3.3}$$

Here i is the natural injection that maps $\boldsymbol{H}^1_0(\Omega)$ into $\boldsymbol{L}^2(\Omega)$. The operator i is retained to draw the attention of the reader to the fact that $\boldsymbol{u}^{k+1}$ and $\hat{\boldsymbol{u}}^{k+1}$ do not a priori live in the same space.

When it comes to discretizing the projection step, the two different frameworks described above yield radically different implementations. The first formulation yields a coupled system for velocity and pressure unknowns, while the second formulation involves only one scalar Poisson problem. However, as shown in Guermond [14] and Guermond and Quartapelle [16], these different frameworks lead to the same convergence estimates for the space/time solution of the projection scheme, so that the choice between them is a matter of computational efficiency. In the following we solve the projection step as a Poisson problem supplemented with homogeneous Neumann boundary condition.

3.2. The Fully Discrete Equations

Within the spectral framework adopted in this paper, once the projected velocity $\hat{\boldsymbol{u}}^k_N$ is substituted with its expression $i\boldsymbol{u}^k_N - \Delta t \nabla p^k_{\hat{N}}$ in (3.1), the viscous substep reads as follows. Find $\boldsymbol{u}^{k+1}_N \in \boldsymbol{X}_{0,N}$ such that, for all $\boldsymbol{v}_N \in \boldsymbol{X}_{0,N}$,

$$\left(\boldsymbol{v}_N, \frac{\boldsymbol{u}^{k+1}_N - \boldsymbol{u}^k_N}{\Delta t}\right) + \nu\big(\nabla \boldsymbol{v}_N, \nabla \boldsymbol{u}^{k+1}_N\big) = (\boldsymbol{v}_N, \boldsymbol{f}^{k+1}) - \big(\boldsymbol{v}_N, \big(\boldsymbol{u}^k_N \cdot \nabla\big)\boldsymbol{u}^k_N\big) - \big(\boldsymbol{v}_N, \nabla p^k_{\hat{N}}\big). \tag{3.4}$$

The spectral approximation of the Poisson problem accounting for incompressibility takes the following form. Find $p^{k+1}_{\hat{N}} \in M_{\hat{N}}$ such that, for all $q_{\hat{N}} \in M_{\hat{N}}$,

$$\big(\nabla q_{\hat{N}}, \nabla p^{k+1}_{\hat{N}}\big) = -(\Delta t)^{-1}\big(q_{\hat{N}}, \nabla \cdot \boldsymbol{u}^{k+1}_N\big). \tag{3.5}$$

Finally, by introducing the selected basis functions, the three algebraic problems for the velocity components and pressure are obtained, as fully reported in [1].

3.3. Stability and Convergence

The convergence properties of the algorithm (3.4)–(3.5) are stated in the following theorem.

THEOREM 2. *If* $(\boldsymbol{u}, p)$, *the solution to* (2.1) *without nonlinear term*, *is smooth enough in space and time*, *the solution to* (3.4)–(3.5) *satisfies the estimates*

$$\max_{0\le k\le K}\Big(\big\|\boldsymbol{u}(t^k) - \boldsymbol{u}^k_N\big\|_{\boldsymbol{L}^2(\Omega)}, \big\|\boldsymbol{u}(t^k) - \hat{\boldsymbol{u}}^k_N\big\|_{\boldsymbol{L}^2(\Omega)}\Big) \le c(\boldsymbol{u}, p, T, \sigma)(\Delta t + N^{-\sigma}),$$

$$\max_{0\le k\le K}\Big(\beta_{N\hat{N}}\big\|p(t^k) - p^k_{\hat{N}}\big\|_{L^2(\Omega)/Z_{\hat{N}}}, \big\|\boldsymbol{u}(t^k) - \boldsymbol{u}^k_N\big\|_{\boldsymbol{H}^1(\Omega)}\Big) \le c(\boldsymbol{u}, p, T, \sigma)\big(\Delta t^{1/2} + N^{1-\sigma}\big).$$

Proof. We just sketch the proof. First we obtain stability of the velocity using a simple energy argument. By repeating this argument and applying it to the velocity increments $\hat{\boldsymbol{u}}_N^{k+1} - \hat{\boldsymbol{u}}_N^k$, one obtains stability in the $\boldsymbol{L}^2$ norm of the approximate time derivative $(\hat{\boldsymbol{u}}_N^{k+1} - \hat{\boldsymbol{u}}_N^k)/\Delta t$. Then, the key argument to obtaining a stability inequality of pressure consists of building a good approximation of the momentum equation, as follows. By adding the equation $\hat{\boldsymbol{u}}^{k+1} = i\boldsymbol{u}^{k+1} - \Delta t \boldsymbol{\nabla} p^{k+1}$ to (3.4), we obtain

$$\left(\boldsymbol{\nabla}\cdot\boldsymbol{v}_N,\, p_{\hat{N}}^{k+1}\right) = \left(\boldsymbol{v}_N,\, \frac{\hat{\boldsymbol{u}}_N^{k+1} - \hat{\boldsymbol{u}}_N^k}{\Delta t}\right) + \nu\left(\boldsymbol{\nabla}\boldsymbol{v}_N,\, \boldsymbol{\nabla}\boldsymbol{u}_N^{k+1}\right) - \left(\boldsymbol{v}_N,\, \boldsymbol{f}^{k+1}\right).$$

Stability of pressure in the quotient norm of $L^2(\Omega)/Z_{\hat{N}}$ follows easily from the LBB inequality (see Rannacher [25], Shen [28], and Guermond [14] for details).

Note that in the proof of stability of pressure, it is not the coercivity of the Poisson operator in (3.5) that is invoked but the inf-sup inequality (2.5). This remark is the touchstone of this paper.

The results above can be extended to the nonlinear case, provided $\Delta t \le c(\boldsymbol{u}_0, \boldsymbol{f})N^{-2}$. Note that the convergence on pressure is guaranteed only in the quotient norm of $L^2(\Omega)/Z_{\hat{N}}$ and the constant in the error bound is proportional to $1/\beta_{N\hat{N}}$. That is to say, the convergence property of the nonincremental projection method (3.4)–(3.5) is controlled by the ability of the spectral framework to approximate correctly the *steady* Stokes problem.

4. THE BDF INCREMENTAL PROJECTION METHOD

We consider now a second-order incremental projection method, whose theoretical analysis was given in Guermond and Quartapelle [16] and Guermond [15]. This method is known to be more accurate than the nonincremental one for any value of the time step. We see in this case also that the LBB condition of the steady Stokes problem (2.4) controls the convergence in space of the method, although this condition may not seem to be necessary a priori.

4.1. BDF Time Discretization

The incremental version of the fractional-step method consists of making explicit the pressure at the viscous step and correcting it at the projection step, while retaining the complete uncoupling of viscous diffusion from incompressibility. We consider a second-order scheme based on BDF, thoroughly studied in Guermond [15]. The algorithm reads as follows.

Set $\boldsymbol{u}^0 = \boldsymbol{u}_0$ and assume p^0 to be known. At the first time step ($k = 0$), use the incremental projection scheme based on the Euler time discretization to determine the first velocity $\boldsymbol{u}^1$ and pressure p^1. In other words, solve the viscous diffusion problem

$$\begin{cases} \left(\frac{\boldsymbol{v},\boldsymbol{u}^1 - \boldsymbol{u}^0}{\Delta t}\right) + \nu(\boldsymbol{\nabla}\boldsymbol{v}, \boldsymbol{\nabla}\boldsymbol{u}^1) = (\boldsymbol{v}, \boldsymbol{f}^1) - (\boldsymbol{v}, (\boldsymbol{u}^0\cdot\boldsymbol{\nabla})\boldsymbol{u}^0) + (\boldsymbol{\nabla}\cdot\boldsymbol{v}, p^0), \forall \boldsymbol{v} \in \boldsymbol{H}_0^1(\Omega), \\ \boldsymbol{u}^1{}_{|\partial\Omega} = 0, \end{cases} \tag{4.1}$$

and the incremental Poisson problem

$$(\boldsymbol{\nabla} q, \boldsymbol{\nabla}(p^1 - p^0)) = -(\Delta t)^{-1}(q, \boldsymbol{\nabla}\cdot\boldsymbol{u}^1), \quad \forall q \in H^1(\Omega) \cap L_0^2(\Omega), \tag{4.2}$$

so that the first end-of-step velocity is given by $\hat{\boldsymbol{u}}^1 = i\boldsymbol{u}^1 - \Delta t \boldsymbol{\nabla}(p^1 - p^0)$.

Then, for $k \geq 1$, solve the following two problems. First, consider the diffusion step

$$\begin{cases} \frac{(\boldsymbol{v}, 3\boldsymbol{u}^{k+1}) - (\boldsymbol{v}, 4\hat{\boldsymbol{u}}^k + \hat{\boldsymbol{u}}^{k-1})}{2\Delta t} + \nu(\boldsymbol{\nabla v}, \boldsymbol{\nabla u}^{k+1}) \\ \quad = (\boldsymbol{v}, \boldsymbol{f}^{k+1}) - (\boldsymbol{v}, (\boldsymbol{u}_\star^{k+1} \cdot \boldsymbol{\nabla})\boldsymbol{u}_\star^{k+1}) + (\boldsymbol{\nabla} \cdot \boldsymbol{v}, p^k), \quad \forall \boldsymbol{v} \in \boldsymbol{H}_0^1(\Omega), \\ \boldsymbol{u}^{k+1}{}_{|\partial\Omega} = 0, \end{cases} \tag{4.3}$$

where we have introduced the linearly extrapolated velocity $\boldsymbol{u}_\star^{k+1} = 2\boldsymbol{u}^k - \boldsymbol{u}^{k-1}$. Second, perform the projection step in the following incremental (correction) form:

$$(\boldsymbol{\nabla} q, \boldsymbol{\nabla}(p^{k+1} - p^k)) = -\frac{3}{2\Delta t}(q, \boldsymbol{\nabla} \cdot \boldsymbol{u}^{k+1}), \quad \forall q \in H^1(\Omega) \cap L_0^2(\Omega). \tag{4.4}$$

4.2. Fully Discretized Equations

By introducing finite-element spaces $\boldsymbol{X}_{0,N}$ and $M_{\hat{N}}$ as in Section 2.2, we recast the BDF incremental projection algorithm in weak form. Similarly to the nonincremental scheme, the end-of-step velocity is eliminated from the algorithm. For the BDF method, this elimination requires that special attention be paid to the first two steps, $k = 1$ and $k = 2$, since here different forms of extrapolated pressure are obtained (see [1]). A direct calculation leads to the following weak formulation of the viscous step for $k \geq 3$.

For $k \geq 3$, find $\boldsymbol{u}_N^{k+1} \in \boldsymbol{X}_{0,N}$ such that, for all $\boldsymbol{v}_N \in \boldsymbol{X}_{0,N}$,

$$\begin{aligned} &\left(\boldsymbol{v}_N, \frac{3\boldsymbol{u}_N^{k+1} - 4\boldsymbol{u}_N^k + \boldsymbol{u}_N^{k-1}}{2\Delta t}\right) + \nu\big(\boldsymbol{\nabla v}_N, \boldsymbol{\nabla u}_N^{k+1}\big) \\ &\quad = (\boldsymbol{v}_N, \boldsymbol{f}^{k+1}) - \big(\boldsymbol{v}_N, \big(\boldsymbol{u}_{\star,N}^{k+1} \cdot \boldsymbol{\nabla}\big)\boldsymbol{u}_{\star,N}^{k+1}\big) - \frac{1}{3}\big(\boldsymbol{v}_N, \boldsymbol{\nabla}\big(7p_{\hat{\boldsymbol{N}}}^k - 5p_{\hat{\boldsymbol{N}}}^{k-1} + p_{\hat{\boldsymbol{N}}}^{k-2}\big)\big). \end{aligned} \tag{4.5}$$

And for $k \geq 1$, find $(p_{\hat{\boldsymbol{N}}}^{k+1} - p_{\hat{\boldsymbol{N}}}^k) \in M_{\hat{\boldsymbol{N}}}$ such that, for all $q_{\hat{\boldsymbol{N}}} \in M_{\hat{\boldsymbol{N}}}$,

$$\big(\boldsymbol{\nabla} q_{\hat{\boldsymbol{N}}}, \boldsymbol{\nabla}\big(p_{\hat{\boldsymbol{N}}}^{k+1} - p_{\hat{\boldsymbol{N}}}^k\big)\big) = -\frac{3}{2\Delta t}\big(q_{\hat{\boldsymbol{N}}}, \boldsymbol{\nabla} \cdot \boldsymbol{u}_N^{k+1}\big). \tag{4.6}$$

4.3. Stability and Convergence

The error analysis of [15] extends easily to the spectral framework. Hence, we have the following theorem.

THEOREM 3. *If* $(\boldsymbol{u}, p)$*, the solution to* (2.1) *without nonlinear term, is smooth enough in space and time, the solution to* (4.5)–(4.6) *satisfies the estimates*

$$\left\{ \Delta t \sum_{k=0}^{K} \big\|\boldsymbol{u}(t^k) - \boldsymbol{u}_N^k\big\|_{\boldsymbol{L}^2(\Omega)}^2 + \big\|\boldsymbol{u}(t^k) - \hat{\boldsymbol{u}}_N^k\big\|_{\boldsymbol{L}^2(\Omega)}^2 \right\} \leq c(\boldsymbol{u}, p, T, \sigma)(\Delta t^2 + N^{-\sigma}),$$

$$\max_{0 \leq k \leq K} \big(\beta_{N\hat{N}}\big\|p(t^k) - p_{\hat{N}}^k\big\|_{L^2(\Omega)/Z_{\hat{N}}}, \big\|\boldsymbol{u}(t^k) - \boldsymbol{u}_N^k\big\|_{\boldsymbol{H}^1(\Omega)}\big) \leq c(\boldsymbol{u}, p, T, \sigma)(\Delta t + N^{1-\sigma}),$$

where σ accounts for the regularity of $\boldsymbol{u}$ (cf. Lemma 2). Note that to the extent of the authors' knowledge, second-order accuracy in time has been proved only in the $\boldsymbol{L}^2$ norm of the velocity (see also Shen [30] for proof of convergence with Crank–Nicolson time stepping). Once more, the error estimates of velocity do not depend on the inf-sup constant (i.e., both equal

and unequal polynomial order interpolations yield optimal velocity approximation). On the other hand, the error estimate on pressure is proportional to $1/\beta_{N\hat{N}}$ and the convergence is guaranteed only in the quotient space $L^2(\Omega)/Z_{\hat{N}}$.

5. NUMERICAL RESULTS

Now we investigate numerically whether the error estimates derived above are optimal. Actually, when looking at algorithm (3.4)–(3.5), one observes that the two bilinear forms on the left-hand sides are coercive. Hence, despite the remarks above, one may still think that there is some hidden stabilizing mechanism in the nonincremental projection method that can make it work independently of the LBB condition.

5.1. Analytical Test Case

Let us consider as a test problem the Navier–Stokes equations (2.1) with the analytical solution

$$\begin{cases} u_x = -(\cos x \sin y) g(t), \\ u_y = (\sin x \cos y) g(t), \\ p = -\frac{1}{4}[\cos(2x) + \cos(2y)] g^2(t), \end{cases}$$

where $\Omega = [-1, 1]^2$ and $g(t) = \sin(2t)$. Introducing the velocity in the form $\boldsymbol{u} = \tilde{\boldsymbol{u}}(x, y)\, g(t)$, the source term corresponding to the momentum equation in the Navier–Stokes system reads $\boldsymbol{f} = \tilde{\boldsymbol{u}}(x, y)[g'(t) + 2g(t)/\mathrm{Re}]$.

We make two series of convergence tests with respect to Δt, all with $\mathrm{Re} = 100$. In the first series, we use a $\mathbb{P}_{20}/\mathbb{P}_{20}$ interpolation, whereas in the second series we use $\mathbb{P}_{20}/\mathbb{P}_{18}$. This choice of polynomial orders guarantees that the error in space for this smooth solution is much lower than that induced by time splitting, at least within the range of time steps explored.

The results for the nonincremental method are reported in Fig. 1, where the $l^\infty(0, 1; L^2(\Omega))$ and $l^\infty(0, 1; H^1(\Omega))$ norms of the error of velocity and pressure are plotted.

These results are in full accordance with Theorem 2 and confirm that the velocity approximation is first-order accurate in both error norms, irrespective of the adopted discretization (note that inverse inequalities imply that Δt accuracy of velocity in the $\boldsymbol{L}^2$ norm yields also Δt accuracy in the $\boldsymbol{H}^1$ norm, the constant in the error estimate depending on N). As expected from Theorem 2, the convergence behavior of pressure depends on the approximation adopted. In fact, while for $\mathbb{P}_{20}/\mathbb{P}_{18}$ discretization first-order convergence is observed, for equal-order approximation, some sort of convergence in the $l^\infty(0, 1; L^2(\Omega))$ norm is observed only for time steps *greater* than 10^{-3}, and there is no convergence in the $l^\infty(0, 1; H^1(\Omega))$ norm for all time steps.

Looking again at pressure convergence tests with equal-order approximation for the nonincremental scheme, one may have the feeling that we did not reach the end of the story, for there seems to be convergence in the $l^\infty(0, 1; L^2(\Omega))$ norm for $\Delta t > 10^{-3}$. Actually, this result can be understood in the light of Rannacher's analysis of the nonincremental projection method [25]. Let us recall the key points of the argument for the convenience of the reader. The analysis in [25] shows that the nonincremental projection can be viewed as

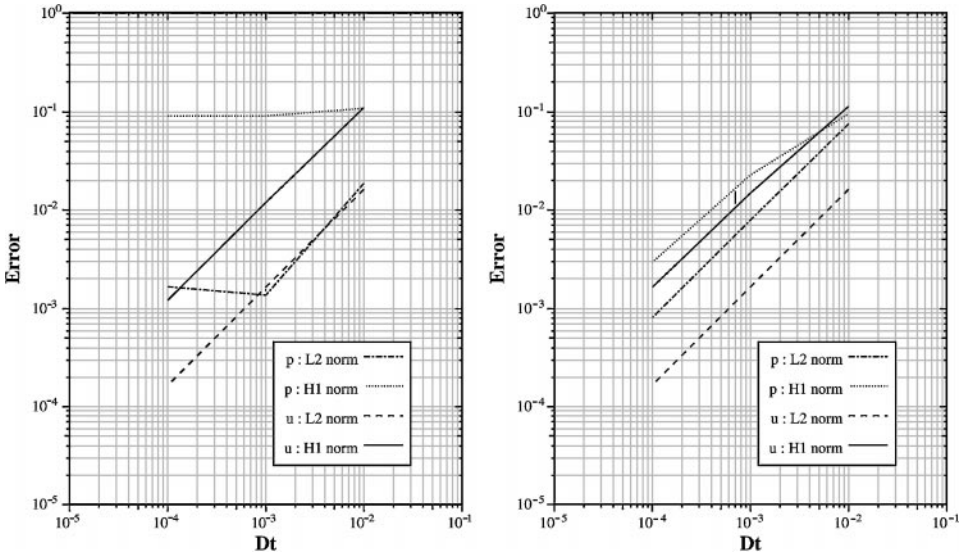

FIG. 1. Convergence behavior for the nonincremental projection method, Re = 100. Equal-order $\mathbb{P}_{20}/\mathbb{P}_{20}$ approximation (left); unequal-order $\mathbb{P}_{20}/\mathbb{P}_{18}$ approximation (right).

a pseudocompressibility technique whose limit problem is

$$\begin{cases} \frac{\partial \boldsymbol{u}_\epsilon}{\partial t} - \nu \nabla^2 \boldsymbol{u}_\epsilon + (\boldsymbol{u}_\epsilon \cdot \boldsymbol{\nabla})\boldsymbol{u}_\epsilon + \boldsymbol{\nabla} p_\epsilon = \boldsymbol{f}, \\ \boldsymbol{\nabla} \cdot \boldsymbol{u}_\epsilon - \epsilon \nabla^2 p_\epsilon = 0, \\ \boldsymbol{u}_{\epsilon|\partial\Omega} = 0, \quad \partial_n p_{\epsilon|\partial\Omega} = 0, \\ \boldsymbol{u}_{|t=0} = \boldsymbol{u}_0, \end{cases} \tag{5.7}$$

where the pseudocompressibility coefficient ϵ is chosen to be Δt in the time discrete case. As a result, some kind of stability of pressure can be expected from the Poisson equation if the time step (i.e., ϵ) is large enough. More precisely, keeping the time continuous in (5.7) but discretizing the space, the pseudocompressibility term yields $\epsilon \int_0^t \|\boldsymbol{\nabla} p_{\hat{N}\epsilon}\|^2_{\boldsymbol{L}^2(\Omega)} ds \le c$. This estimate gives some sort of stability of pressure in the L^2 norm if $\epsilon\, c_i(\hat{N})^2$ is of order 1 or larger, where $c_i(\hat{N})$ is the best constant in the inverse inequality $\|\boldsymbol{\nabla} q_{\hat{N}}\|_{\boldsymbol{L}^2(\Omega)} \le c_i(N)\|q_{\hat{N}}\|_{\boldsymbol{L}^2(\Omega)}$, where $q_{\hat{N}}$ spans $M_{\hat{N}}$. For the two types of discretizations considered in this paper, we have $c_i(\hat{N}) \sim N^2$ (see, e.g., [5, 24]). Hence, in practice, convergence of pressure is observed in the eyeball norm (i.e., the L^2 norm, provided $\Delta t \ge cN^{-4}$). Note, however, that the stability provided by the Poisson equation is not strong enough to keep the spurious modes from lurking, as can be seen in the convergence test in the H^1 norm and on the plot of the error on the pressure field (see Fig. 3, left).

Next we investigate the accuracy properties of the incremental scheme. The initial pressure needed by the algorithm reported in Section 4.1 has been computed using orthogonal projection (in the $L^2(\Omega)$ sense) of $p(t = 0)$ on the subspace spanned by the basis functions for the pressure. On the left side of Fig. 2 we have plotted the convergence curves for $\mathbb{P}_{20}/\mathbb{P}_{20}$ interpolation. The pressure does not converge, even in the weaker $l^\infty(0, 1; L^2(\Omega))$ norm, regardless of the magnitude of the time step. The convergence of velocity is unaffected by the

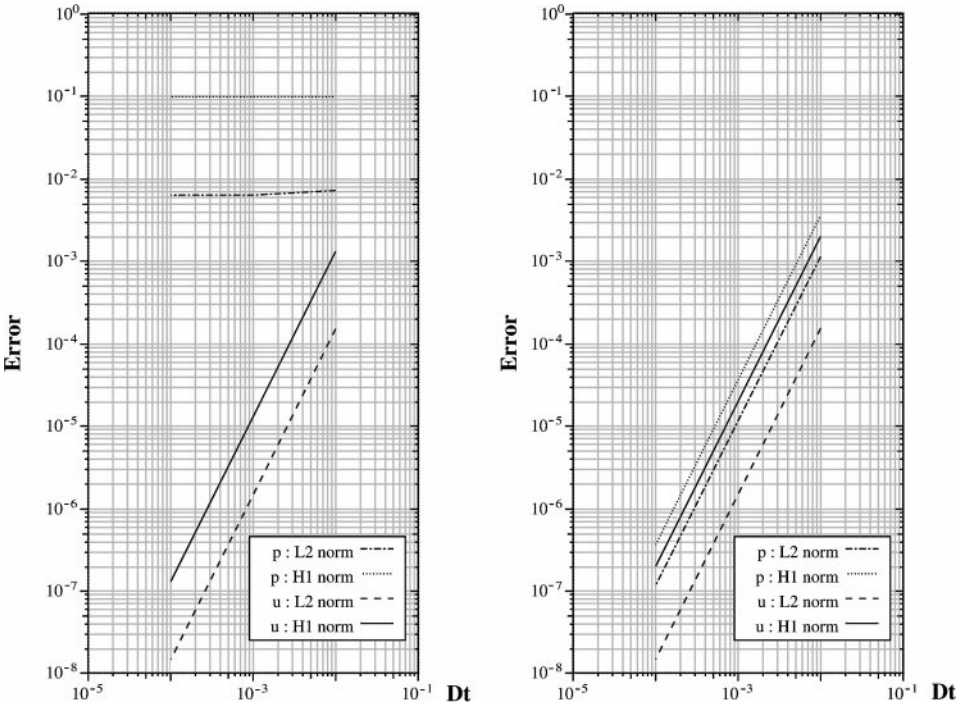

FIG. 2. Convergence behavior for the incremental BDF version of the projection method, Re = 100. Equal-order $\mathbb{P}_{20}/\mathbb{P}_{20}$ approximation (left); unequal-order $\mathbb{P}_{20}/\mathbb{P}_{18}$ approximation (right).

kind of discretization. The convergence curves for the unequal order $\mathbb{P}_{20}/\mathbb{P}_{18}$ interpolation are plotted on the right of Fig. 2. Both velocity and pressure converge with second-order rate in both error norms. These convergence tests clearly show that, for the incremental projection algorithm considered here, a compatible discretization is mandatory for pressure to converge.

Similarly to what is observed for equal-order finite-element spatial discretizations, the lack of convergence of pressure for both the nonincremental and the incremental schemes is due to the insurgence of spurious modes. In Fig. 3, we show error fields of pressure at $t = 1$ obtained using the nonincremental scheme with $\Delta t = 0.00001$ for $\mathbb{P}_{20}/\mathbb{P}_{20}$ and $\mathbb{P}_{20}/\mathbb{P}_{18}$ interpolations. The same quantities, but for the incremental scheme with $\Delta t = 0.01$ and $\mathbb{P}_{40}/\mathbb{P}_{40}$ and $\mathbb{P}_{40}/\mathbb{P}_{38}$ interpolations, are shown in Fig. 4.

The checkerboard pattern of the spurious pressure modes on the equal-order approximation is evident for the two projection methods considered.

Note also that, in accordance with the analysis of [25], a numerical boundary layer is observable on the nonincremental $\mathbb{P}_{20}/\mathbb{P}_{18}$ results. This boundary layer is the direct consequence of the enforcement of the nonrealistic Neuman condition $\partial_n p = 0$ on $\partial\Omega$. This boundary layer does not show up on the spatial distribution of the error of pressure obtained with the incremental scheme with the $\mathbb{P}_{40}/\mathbb{P}_{38}$ interpolation.

To finish this section, we add that we have also done space convergence tests with respect to the polynomial order N, δt being chosen sufficiently small so that the space error dominates. As stated in Theorems 2 and 3, we observed spectral accuracy for both schemes with $\mathbb{P}_N/\mathbb{P}_{N-2}$ interpolation.

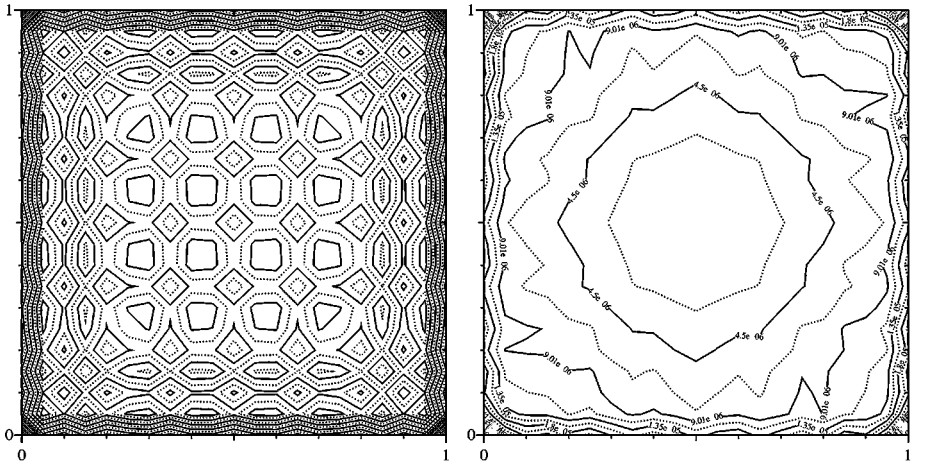

FIG. 3. Nonincremental scheme, pressure error field at $t = 1$, $\Delta t = 0.00001$, Re $= 100$. (Left) Equal-order $\mathbb{P}_{20}/\mathbb{P}_{20}$ interpolation; (right) different-order $\mathbb{P}_{20}/\mathbb{P}_{18}$ interpolation.

5.2. Driven Cavity Problem

We now consider the solution of the driven cavity problem [10] with a Reynolds number Re $= 100$. In this problem, the horizontal component of velocity is discontinuous in the two upper corners, being equal to one on the top side and equal to zero on the other sides, while the vertical component is zero on the four sides. In the calculation of the lifting of the Dirichlet datum, the horizontal velocity in the top corners has been set to zero to avoid any mass flux through the vertical walls of the cavity. Moreover, the initial velocity and pressure fields employed in the incremental method have been set to zero.

The pressure fields obtained by the nonincremental scheme at $t = 10$, computed with $\mathbb{P}_{40}/\mathbb{P}_{40}$ interpolation and with two different time steps, $\Delta t = 0.01$ and $\Delta t = 0.00001$, are shown in Fig. 5.

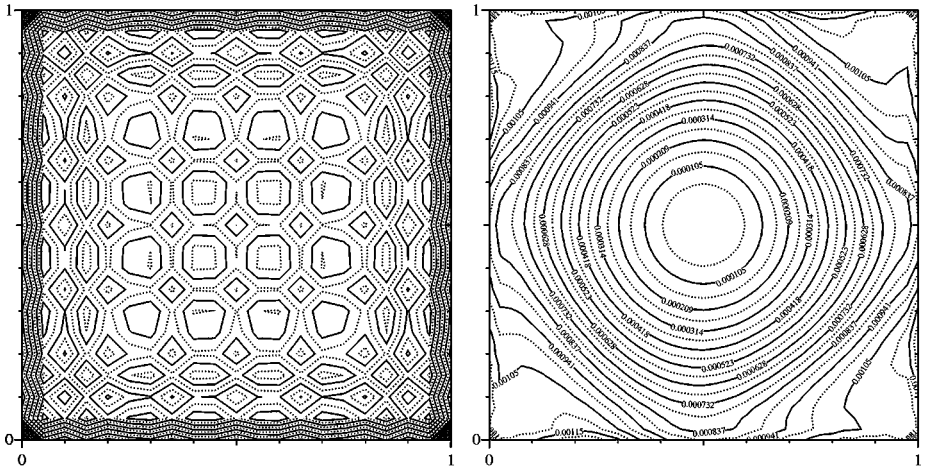

FIG. 4. Incremental projection method, pressure error field at $t = 1$, $\Delta t = 0.01$, Re $= 100$. (Left) $\mathbb{P}_{40}/\mathbb{P}_{40}$ interpolation; (right) $\mathbb{P}_{40}/\mathbb{P}_{38}$ interpolation.

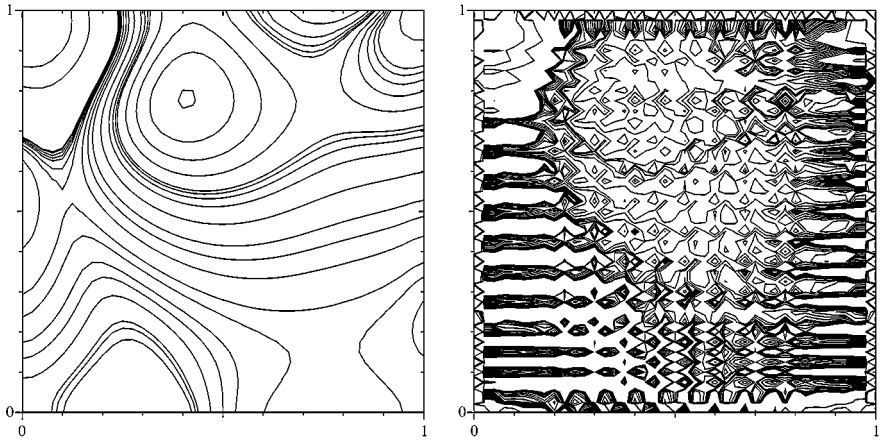

FIG. 5. Pressure field in the driven cavity for Re $= 100$: at $t = 10$. Nonincremental method with $\mathbb{P}_{40}/\mathbb{P}_{40}$ interpolation. $\Delta t = 0.01$ (left) and $\Delta t = 0.00001$ (right).

The wild oscillations observed with $\Delta t = 0.00001$ confirm the need to satisfy the inf–sup condition to obtain an accurate solution, while the apparent smoothness of the solution obtained with $\Delta t = 0.01$ shows the already-mentioned stabilizing effect of the nonconsistent Poisson equation for time steps large enough.

Still using the nonincremental projection method but choosing polynomial bases that respect the LBB condition (e.g., $\mathbb{P}_{40}/\mathbb{P}_{38}$ interpolation) yields pressure fields that are free of any spurious modes, as shown in Fig. 6. Note however that some oscillations can be observed close to the boundary for the smaller time step $\Delta t = 0.00001$. These oscillations are triggered by singularities localized at the cavity corners and are known in the literature as the Gibbs phenomenon. Similar oscillations are found also when using the vorticity and stream function formulation [2]. They can be eliminated by subtracting the singularity, as explained below. Note that these oscillations do not show up when $\Delta t = 0.01$, since in this case Δt is large enough for the regularization effects of the nonconsistent Poisson equation, already mentioned above, to be significant.

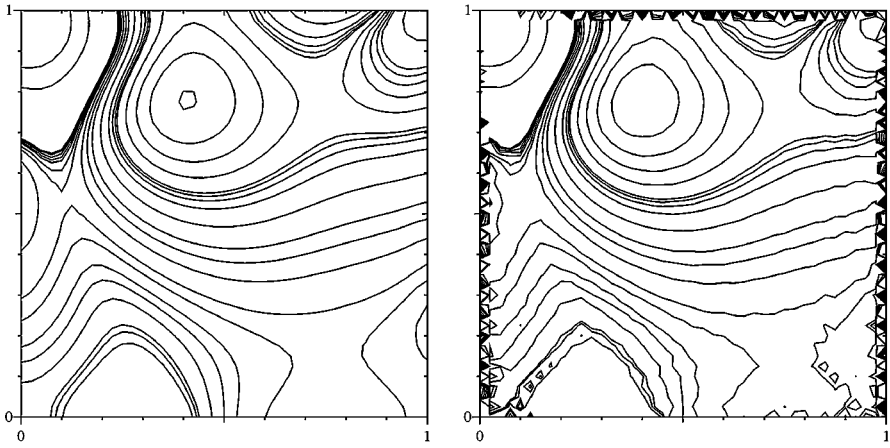

FIG. 6. Pressure field in the driven cavity for Re $= 100$ at $t = 10$. Nonincremental method with different-order $\mathbb{P}_{40}/\mathbb{P}_{38}$ interpolation. (Left) $\Delta t = 0.01$; (right) $\Delta t = 0.00001$. The spatial oscillations localized near the boundary for $\Delta t = 0.00001$ are due to a Gibbs phenomenon induced by the solution's singularity.

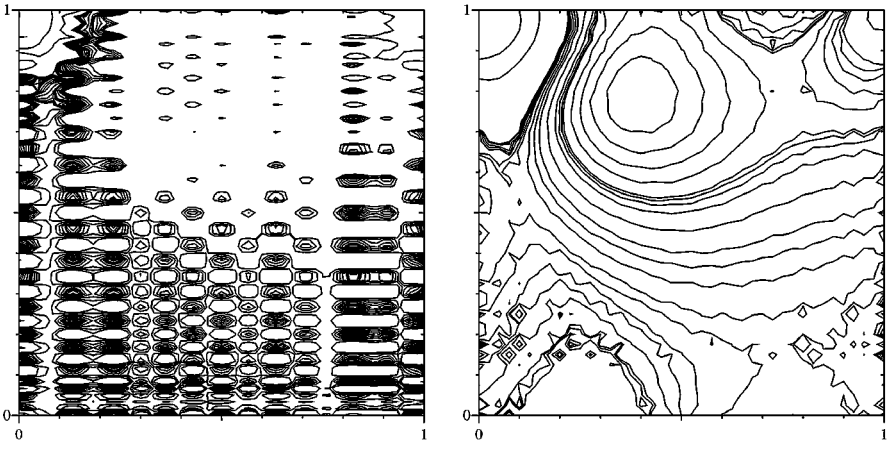

FIG. 7. Pressure field in the driven cavity for Re $= 100$, $t = 10$. Incremental projection method, $\Delta t = 0.01$. (Left) $\mathbb{P}_{40}/\mathbb{P}_{40}$ interpolation; (right) $\mathbb{P}_{40}/\mathbb{P}_{38}$ interpolation.

Now we analyze the performance of the incremental BDF scheme. The pressure fields computed using this scheme at $t = 10$ with $\Delta t = 0.01$ for $\mathbb{P}_{40}/\mathbb{P}_{40}$ and $\mathbb{P}_{40}/\mathbb{P}_{38}$ interpolations are shown in Fig. 7. Spurious modes are clearly visible on the $\mathbb{P}_{40}/\mathbb{P}_{40}$ results (left) whereas the pressure field obtained with the $\mathbb{P}_{40}/\mathbb{P}_{38}$ (right) approximation looks reasonable. This test confirms that the incremental method does not work properly for pressure unless the LBB condition is satisfied, as suggested in Theorem 3.

Note once more that, for the $\mathbb{P}_{40}/\mathbb{P}_{38}$ result, some oscillations are visible close to the cavity boundary. As explained above, they are the manifestation of the Gibbs phenomenon induced by the two singularities localized at the cavity corners. Following the technique presented by Botella and Peyret for the primitive variable formulation [6, 7], which amounts to solving the problem for auxiliary variables with singular components removed, we were able to eliminate such oscillations, as presented in Fig. 8.

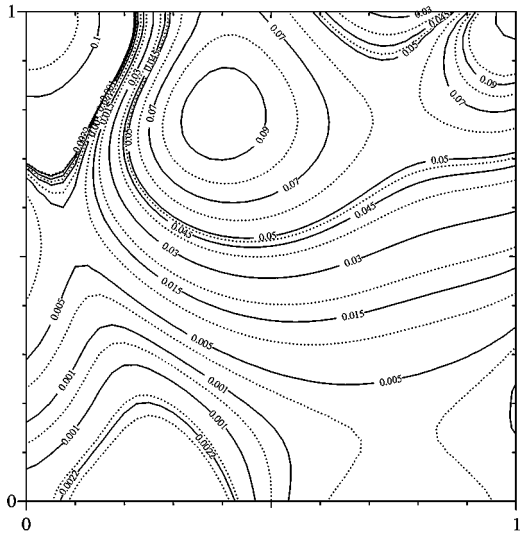

FIG. 8. Pressure field in the driven cavity for Re $= 100$ at $t = 10$ obtained using the singularity subtraction technique and the incremental projection method, $\mathbb{P}_{40}/\mathbb{P}_{38}$ interpolation, and $\Delta t = 0.01$.

In conclusion, the two series of tests performed above clearly confirm that the LBB condition of the steady Stokes problem (2.4) controls the convergence of both the nonincremental and incremental projection technique.

6. CONCLUSIONS

This paper has investigated the relevance of the LBB condition in spectral projection methods. We have considered the stability and convergence properties of a first-order nonincremental projection method and a second-order incremental projection method, both based on spectral Galerkin–Legendre spatial discretization.

The argumentation developed in the present paper is fourfold.

1. The nonincremental projection method falls in the class of pseudocompressibility techniques, provided the time step is not too small (i.e., $\Delta t \geq cN^{-4}$). Under this circumstance only, equal-order polynomial approximation can be used. But even in this case, we have shown numerically that the $\mathbb{P}_N/\mathbb{P}_{N-2}$ interpolation is more accurate than the equal-order approximation.

2. For the nonincremental method with very small time steps and for the incremental one for all time steps, we have shown that stability and convergence in space is controlled by the ability of the spectral discretization to approximate the steady Stokes problem. That is to say, even though the two substeps of the two projection methods considered are coercive, the global convergence is controlled by the LBB constant of the steady Stokes problem.

3. In accordance with a striking approximation result of the steady Stokes problem by Sacchi-Landriani and Vandeven [27], we have shown that equal-order polynomial spectral approximations yield optimal error estimates of velocity in all circumstances but is generally not optimal for pressure.

4. For the two projection methods considered in this paper, mixed $\mathbb{P}_N/\mathbb{P}_{N-2}$ approximation always yields the same space accuracy as that of the steady Stokes problem, whereas for $\mathbb{P}_N/\mathbb{P}_N$ approximation this property holds only in a quotient space (i.e., the correct pressure field can be recovered only by adequate postprocessing, as suggested in [5]).

ACKNOWLEDGMENTS

The question evoked in the paper's title was brought to the authors' attention by Luigi Quartapelle. They are grateful to him for his constant support and fruitful discussions that greatly improved the content of the paper.

REFERENCES

1. F. Auteri and N. Parolini, Mixed-basis spectral projection method, *J. Comput. Phys*., in press.
2. F. Auteri and L. Quartapelle, Galerkin spectral method for the vorticity and stream function equations, *J. Comput. Phys*. **149**, 306 (1999).
3. M. Azaiez, *Calcul de la pression dans le problème de Stokes pour les fluides visqueux incompressibles par une méthode spectrale de collocation*, Ph.D. thesis (Université Paris XI, Orsay, France, 1990).
4. I. Babuška, The finite element method with Lagrangian multipliers, *Numer. Math*. **20**, 179 (1973).
5. C. Bernardi and Y. Maday, *Approximations spectrales des problèmes aux limites elliptiques* (Springer-Verlag, Paris, 1992).
6. O. Botella, On the solution of the Navier–Stokes equations using Chebyshev projection schemes with third-order accuracy in time, *Comput. Fluids* **26**, 107 (1997).

7. O. Botella and R. Peyret, Benchmark spectral results on the lid-driven cavity flow, *Comput. Fluids* **27**, 421 (1998).
8. F. Brezzi, On the existence uniqueness and approximation of saddle-point problems arising from Lagrangian multipliers, Revue Française d' Automatique, d' Informatique et de Recherche Operationnelle **R.2**, 129 (1974).
9. F. Brezzi and M. Fortin, *Mixed and Hybrid Finite Element Methods*, Springer Series in Computational Mathematics (Springer-Verlag, New York, 1991), Vol. 15.
10. O. R. Burggraf, Analytical and numerical studies of the structure of steady separated flows, *J. Fluid Mech.* **24**, 113 (1966).
11. C. Canuto, M. Y. Hussaini, A. Quarteroni, and T. A. Zang, *Spectral Methods in Fluid Mechanics* (Springer-Verlag, New York, 1988).
12. A. J. Chorin, Numerical solution of the Navier–Stokes equations, *Math. Comput*. **22**, 745 (1968).
13. A. J. Chorin, On the convergence of discrete approximations to the Navier–Stokes equations, *Math. Comput.* **23**, 341 (1969).
14. J.-L. Guermond, Some implementations of projection methods for Navier–Stokes equations, *Modél. Math. Anal. Numér*. **30**, 637 (1996).
15. J.-L. Guermond, Un résultat de convergence à l'ordre deux en temps pour l'approximation des équations de Navier–Stokes par une technique de projection, *Modél. Math. Anal. Numér.* **33**, 169 (1999).
16. J.-L. Guermond and L. Quartapelle, On the approximation of the unsteady Navier–Stokes equations by finite element projection methods, *Numer. Math*. **80**, 207 (1998).
17. J.-L. Guermond and L. Quartapelle, On stability and convergence of projection method based on pressure Poisson equation, *Int. J. Numer. Meth. Fluids* **26**, 1039 (1998).
18. T. J. R. Hughes, L. P. Franca, and M. Balestra, A new finite element formulation for computational fluid dynamics: V. Circumventing the Babuska-Brezzi condition: A stable Petrov-Galerkin formulation of the Stokes problem accommodating equal-order interpolations, *Comput. Meth. Appl. Mech. Eng.* **63**, 85 (1986).
19. H. O. Kreiss and J. Oliger, Stability of the Fourier method, *SIAM J. Numer. Anal*. **16**, 421 (1979).
20. O. A. Ladyshenskaya, *The Mathematical Theory of Viscous Incompressible Flow*, 2nd ed. (Gordon and Breach, New York, 1969).
21. J. M. Lopez and Jie Shen, An efficient spectral-projection method for the Navier–Stokes Equations in cylindrical geometries I: axisymmetric cases, *J. Comput. Phys*. **139**, 308 (1998).
22. Y. Maday, D. Meiron, A. T. Patera, and E. M. Rønquist, Analysis of iterative methods for the steady and unsteady Stokes problem: Application to spectral element discretizations, *SIAM J. Sci. Comput*. **14**, 310 (1993).
23. S. A. Orzag, Comparison of pseudo-spectral and spectral approximations, *Stud. Appl. Math*. **51**, 253 (1972).
24. A. Quarteroni and A. Valli, *Numerical Approximation of Partial Differential Equations*, Springer Series in Computational Mathematics (Springer-Verlag, New York, 1994), Vol. 23.
25. R. Rannacher, On Chorin's projection method for the incompressible Navier–Stokes equations, in *Lectures Notes in Mathematics* (Springer-Verlag, Berlin, 1992), Vol. 1530, pp. 167–183.
26. E. M. Rønquist, *Optimal Spectral Element Methods for the Unsteady 3-Dimensional Incompressible Navier–Stokes Equations*, Ph.D. thesis (Massachusetts Institute of Technology, Boston, 1988).
27. G. Sacchi-Landriani and H. Vandeven, Polynomial approximation of divergence-free functions, *Math. Comput.* **52**, 103 (1989).
28. J. Shen, On error estimates of the projection methods for Navier–Stokes equations: First-order schemes, *SIAM J. Numer. Anal*. **29**, 57 (1992).
29. J. Shen, Efficient spectral-Galerkin method. I. Direct solvers of second- and fourth-order equations using Legendre polynomials, *SIAM J. Sci. Comput.* **15**, 1489 (1994).
30. J. Shen, On error estimates of the projection methods for Navier–Stokes equations: Second-order schemes, *Math. Comput*. **65**, 1039 (1996).
31. R. Temam, Sur l'approximation de la solution des équations de Navier–Stokes par la méthode de pas fractionnaires, *Arch. Rat. Mech. Anal*. **33**, 377 (1969).
32. R. Temam, *Navier–Stokes Equations*, Studies in Mathematics and Its Applications (North-Holland, Amsterdam, 1977), Vol. 2.